International Journal of Vehicle Safety

ISSN online: 1479-3113 - ISSN print: 1479-3105
https://www.inderscience.com/ijvs

Driving safety of articulated vehicle on a typical interchange

Shuang Luo, Guiyuan Chen, Jin Xu

DOI: 10.1504/IJVS.2022.10054757

Article History:

Received:	02 November 2021
Accepted:	10 February 2022
Published online:	17 March 2023

Driving safety of articulated vehicle on a typical interchange

Shuang Luo*, Guiyuan Chen and Jin Xu

College of Traffic and Transportation,
Chongqing Jiaotong University,
Nan'an District, Chongqing, China
Email: sluo410k@foxmail.com
Email: chenguiyuan0227@163.com
Email: yhnl272727@163.com
*Corresponding author

Abstract: Road conditions at interchanges are more complicated than those on basic freeway segments, which results in high probability of risky situations. To simulate the driving safety of an articulated vehicle on a typical interchange, a virtual vehicle model is developed and validated. Driving simulations are conducted on each ramp of the interchange. Influences of longitudinal velocity and road friction are discussed. The results show that the lateral accelerations increase with increased driving speed or decreased curve radius. The articulated vehicle body rolls to the inside of the circular curves and transition curves, and the roll angles increase with the decrease in speed. The low-speed heavy vehicle might roll over to the inside of the large banked curves. The allowed driving speeds are decreased and the critical speeds for sideslip are obtained at low friction conditions. Accident prevention methods are suggested to enhance the driving safety on the interchange.

Keywords: articulated vehicle; interchange; ramp; driving safety; roll stability; lateral acceleration; road friction; bank angle; 5-degrees-of-freedom model; TruckSim.

Reference to this paper should be made as follows: Luo, S., Chen, G. and Xu, J. (2022) 'Driving safety of articulated vehicle on a typical interchange', *Int. J. Vehicle Safety*, Vol. 12, Nos. 3/4, pp.307–321.

1 Introduction

Interchanges are essential components and important transportation junctions of a freeway. The length of the interchange is less than 5% of the whole mileage of the freeway (Hu et al., 2020). However, more than 30% of the traffic accidents on freeways occurred here (Luo et al., 2017). This is mainly due to improper running speed and uncertain road information. Vehicle longitudinal velocity greatly exceeds the designed index on the ramps after driving at a high speed onto the ramps from the motorway without braking enough, which will result in instability of the vehicle and cause accidents.

Driving safety on ramps was investigated by vehicle driving test, naturalistic data from video images and simulation. In driving tests, numbers of experienced and skilful drivers are employed as volunteers, and Inertial Measurement Unit (IMU) is utilised to record the driving trajectory, moving speed and accelerations. Xu et al. (2019a and 2019b) investigated lateral acceleration and longitudinal velocity characteristics of passenger cars on helical ramps. The driving tests were conducted using 4 different business cars. The IMU and GPS were combined to measure vehicle operating characteristics. Based on these data, speed pattern and acceleration pattern were determined on the ramps. They concluded that the longitudinal velocity of passenger cars is positively while the lateral acceleration is negatively correlated with the ramp radius. In another study by Xu et al. (2019c) analysed driving behaviours at the entrance and exit of clover leaf interchanges according to experimental longitudinal velocity and acceleration. Based on these, they suggested the start and the end of safe deceleration and acceleration length by statistics. Ding et al. (2021) specified running status of passenger cars on roundabout ramps using running speed, longitudinal and lateral acceleration. The authors found that the deceleration section for turns and acceleration section for exits are highly risky sections of dangerous driving behaviour. Lyu et al. (2018) obtained vehicle trajectories, section speed profiles and lane position from driving tests in which 46 volunteers participated on a typical exit ramp. Thereafter, they analysed lane-change characteristics and speed distribution of the drivers with different genders, occupations and driving experiences to reduce traffic accidents on these ramps.

Vehicle operating characteristics could be extracted by data processing software from the video images which are taken from traffic cameras, hovering helicopters or unmanned aerial vehicles. Polus et al. (1985) and Livneh et al. (1988) recorded states of motion for vehicles at the entrance/exit of interchanges, and obtained the location distribution of merging/diverging places coupled with the acceleration/deceleration distances. Farah et al. (2019) proposed a prediction model considering road curve radius, bank angle, lane width and shoulder width, to estimate vehicle operating speed during ramp design process. In a further study, the authors chose free-moving vehicles on different interchanges as subjects from video images (Farah et al., 2017). They collected trajectory and velocity information of individual vehicle, and provide an insight into speed patterns along different type of ramps while approaching and negotiating the ramp curves. Kim (2010) examined lane changing points, speed distributions and deceleration characteristics for four exit ramps, and found traffic accidents happened most potentially at transition curves by analysing accident data on ramps.

Simulation depends on driving simulators and dynamics software. Calvi et al. (2012, 2015, 2020) explained the crash causes and analysed influencing factors of trajectory and speed along acceleration and deceleration lanes by driving performance studies on a simulator. Portera and Bassani (2020) carried out driving simulation experiments in which 48 participants were employed and separated into groups according to age and gender. Vehicle longitudinal velocities and lateral positions were investigated considering different ramp radius, length, curve direction and traffic conditions. Dynamics analysis software is necessary for virtual simulation, for instance ADAMS, CarSim and TruckSim, which is also used to analyse and evaluate driving safety and operating characteristics of vehicles. Dou et al. (2020a, 2020b) developed a dynamics model of a passenger car, and studied driving safety and comfort on the ramps of a bell-bottomed interchange and a clover leaf interchange under different running speed. Afterwards, the authors discussed influences of the radius of curves. Liu et al. (2014)

simulated entrance ramp system considering driver's behaviour characteristics. They obtained traffic flow and running speed at the entrance, based on which driving safety was analysed.

The above-mentioned literatures are all aimed at the driving safety of passenger cars, seldom involving heavy commercial vehicles, such as articulated vehicles. The articulated vehicle transversally skids or rolls over during travelling on large curvature road at a high speed. The traffic on ramps will be obstructed after articulated vehicle accidents occurred because of long vehicle body size, which is more serious than that of the passenger cars. The present study is to study the driving safety of the articulated vehicle on a typical interchange. For this purpose, a linear 5-degrees-of-freedom (DOF) vehicle model is developed, and employed to validate the virtual prototype model built by TruckSim software. The interchange model is established, and driving simulations on each ramp are carried out under different speed and road friction conditions.

2 Simulation model

2.1 5-DOF model of articulated vehicle

To develop the 5-DOF yaw-roll model of the heavy commercial vehicle with a tractor unit and a semi-trailer, the following assumptions are made:

1) Three axles of the semi-trailer are simplified into a single axle of which the longitudinal position is located at the geometry of centre of the previous three axles.

2) The articulated angle is small and can be neglected.

3) The hitch transfers lateral force and roll moment only.

The 5-DOF vehicle model is illustrated in Figure 1. The model involves lateral, yaw and roll motion of the tractor unit, coupled with yaw and roll motion of the semi-trailer. The variables and the corresponding nomenclatures in the following equations are presented in the appendix.

The differential equations of motion for the tractor unit are given by

$$\begin{aligned}
&m_{\mathrm{q}}u\left(\dot{\beta}_{\mathrm{q}}+\gamma_{\mathrm{q}}\right)-m_{\mathrm{sq}}h_{\mathrm{sq}}\ddot{\varphi}_{\mathrm{q}}=F_{\mathrm{fq}}+F_{\mathrm{rq}}-F_{\mathrm{qb}}\\
&I_{z\mathrm{q}}\dot{\gamma}_{\mathrm{q}}-I_{xz\mathrm{q}}\ddot{\varphi}_{\mathrm{q}}=F_{\mathrm{fq}}a_1-F_{\mathrm{rq}}a_2+F_{\mathrm{qb}}a_{\mathrm{o}}\\
&I_{x\mathrm{sq}}\ddot{\varphi}_{\mathrm{q}}-m_{\mathrm{sq}}h_{\mathrm{sq}}u\left(\dot{\beta}_{\mathrm{q}}+\gamma_{\mathrm{q}}\right)=m_{\mathrm{sq}}gh_{\mathrm{sq}}\varphi_{\mathrm{q}}-K_{\mathrm{q}}\varphi_{\mathrm{q}}-C_{\mathrm{q}}\dot{\varphi}_{\mathrm{q}}+F_{\mathrm{qb}}h_{\mathrm{crq}}+K_{\mathrm{qb}}\left(\varphi_{\mathrm{q}}-\varphi_{\mathrm{b}}\right)
\end{aligned}\tag{1}$$

The mathematical expressions of the semi-trailer model are shown as follows:

$$\begin{aligned}
&m_{\mathrm{b}}u\left(\dot{\beta}_{\mathrm{b}}+\gamma_{\mathrm{b}}\right)-m_{\mathrm{sb}}h_{\mathrm{sb}}\ddot{\varphi}_{\mathrm{b}}=F_{\mathrm{b}}+F_{\mathrm{qb}}\\
&I_{z\mathrm{b}}\dot{\gamma}_{\mathrm{b}}-I_{xz\mathrm{b}}\ddot{\varphi}_{\mathrm{b}}=F_{\mathrm{qb}}b_{\mathrm{o}}-F_{\mathrm{b}}b_1\\
&I_{x\mathrm{sb}}\ddot{\varphi}_{\mathrm{b}}-m_{\mathrm{sb}}h_{\mathrm{sb}}u\left(\dot{\beta}_{\mathrm{b}}+\gamma_{\mathrm{b}}\right)=m_{\mathrm{sb}}gh_{\mathrm{sb}}\varphi_{\mathrm{b}}-K_{\mathrm{b}}\varphi_{\mathrm{b}}-C_{\mathrm{b}}\dot{\varphi}_{\mathrm{b}}-F_{\mathrm{qb}}h_{\mathrm{crb}}-K_{\mathrm{qb}}\left(\varphi_{\mathrm{q}}-\varphi_{\mathrm{b}}\right)
\end{aligned}\tag{2}$$

Figure 1 5-DOF model of the articulated vehicle

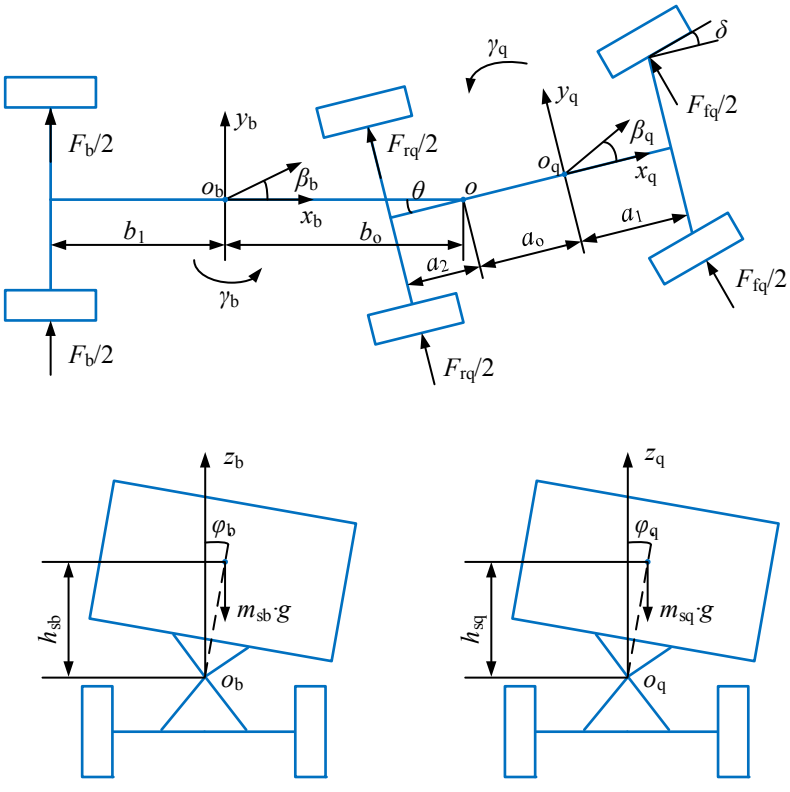

And

$$\dot{\beta}_b = \dot{\beta}_q - \frac{h_{crq}\ddot{\varphi}_q}{u} + \frac{h_{crb}\ddot{\varphi}_b}{u} - \frac{a_o\dot{\gamma}_q}{u} - \frac{b_o\dot{\gamma}_b}{u} + \gamma_q - \gamma_b \tag{3}$$

The lateral force of each tyre can be calculated based on the linear assumption and given by

$$\begin{cases} F_{fq} = k_{fq}\alpha_{fq} \\ F_{rq} = k_{rq}\alpha_{rq} \\ F_b = k_b\alpha_b \end{cases} \tag{4}$$

Here, the slip angles of each tyre are expressed as

$$\begin{cases} \alpha_{fq} = \beta_q + \dfrac{a_1\gamma_q}{u} - \delta \\ \alpha_{rq} = \beta_q - \dfrac{a_2\gamma_q}{u} \\ \alpha_b = \beta_b - \dfrac{b_1\gamma_b}{u} \end{cases} \tag{5}$$

2.2 TruckSim model of articulated vehicle

To simulate lane change during approaching and negotiating the interchange, and observe the vehicle trajectories as well as animations, a virtual prototype model is generated in TruckSim software based on a Dongfeng heavy commercial vehicle, as shown in Figure 2. The configuration of the vehicle is specified as 'S_S+SSS', where 'S_S' indicates a two-axle tractor, and 'SSS' a three-axle semi-trailer (Brown et al., 2020). The tractor consists of a front steer axle, a rear drive axle, suspension sub-system, steering subsystem, braking subsystem, powertrain and sprung mass. The semi-trailer is modelled including three braked trailer axles, leaf spring and sprung mass. The two components are connected by a fifth-wheel.

Figure 2 TruckSim model of the articulated vehicle

2.3 Model validation

A double-lane change manoeuvre is performed to evaluate the validity of the virtual prototype model. The articulated vehicle is driven on fine road with friction coefficient of 0.85 at a constant speed of 50 km/h; the steering wheel angle is modulated to track the reference path, and the lateral accelerations, yaw rates and roll angles are measured, as shown in Figure 3. The responses derived from the TruckSim model show good agreements with the results obtained by the 5-DOF linear model, except small mismatches in the yaw rate of the semi-trailer.

2.4 Road model

Shuangqiao interchange designed as a trumpet type is located on Naqian freeway in Sichuan province, China. This interchange starts from section marked NK71+000, and ends at NK72+580. Four ramps are interlinked with the basic freeway segments, in which Ramp-A and -D are off-ramps, and Ramp-B and -C are on-ramps, as shown in Figure 4. Curve elements of the interchange ramps are shown in Table 1. Global X-Y coordinates of path are imported into TruckSim software to build the 3-dimensional roads. Moreover, the road slopes and banks are involved.

Figure 3 Model validation

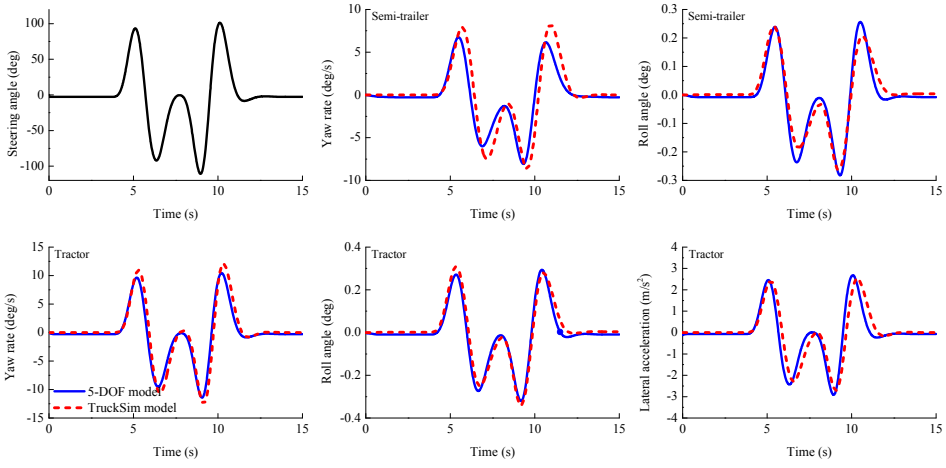

Figure 4 Interchange configuration

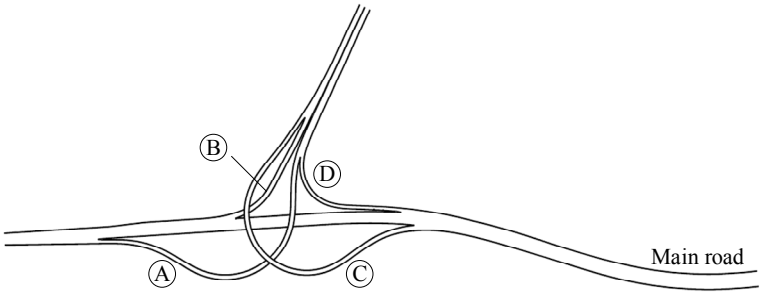

Table 1 Main feature of each ramp

Road name	*Curve length (m)*	*Minimum radius (m)*	*Maximum slope*	*Maximum bank*
Main lane	1580	800	4.98%	3%
Ramp-A	1064	140	–5.73%	5%
Ramp-B	610	125	–4.06%	6%
Ramp-C	971	125	4.33%	6%
Ramp-D	759	85	–3.77%	6%

3 Simulation and results

Driving simulations are conducted, from the main lane to ramp-A, individually from ramp-B and ramp-C to the main lane, and from the main lane to ramp-D. To demonstrate the entire lane change, start station of each simulation is set far enough away from the ramp entrance and end station the ramp exit.

3.1 Effect of speed

Although the speed limitation is 40 km/h on ramps, most of vehicles are driven with higher speed than the allowed. Therefore, the target longitudinal speed is defined as 30, 40, 50, 60 and 80 km/h on the road. The road friction coefficient is 0.6.

3.1.1 On ramp-A

When the articulated vehicle is driven from the main lane to the ramp-A, the steering angle is shown in Figure 5(a). This indicates the driver constantly adjusts the steering wheel to accommodate the road alignment changes. When the vehicle arrives at the circular curve with the minimum radius of the ramp-A, the steering angle maintain the maximum coupled with the lateral acceleration, as presented in Figure 5(b). The driving station there is 425 to 650 m. The lateral acceleration increases with the increased vehicle speed. The steady-stable lateral acceleration of the semi-trailer on this road segment is 0.45, 0.88, 1.38, 1.99 and 3.54 m/s^2 at the speed of 30, 40, 50, 60 and 80 km/h, respectively. The extrema of the lateral acceleration occur at circular curves with the radius of 210 m, 140 m and 240 m, individually. The response of the semi-trailer is close to that of the tractor, but the former lags slightly.

Figure 5 Steering wheel angle and lateral acceleration on ramp-A (a) Steering wheel angle (b) Lateral acceleration

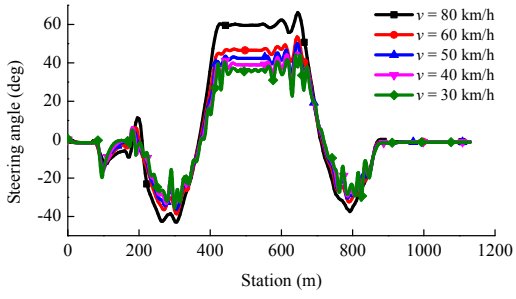

(a)

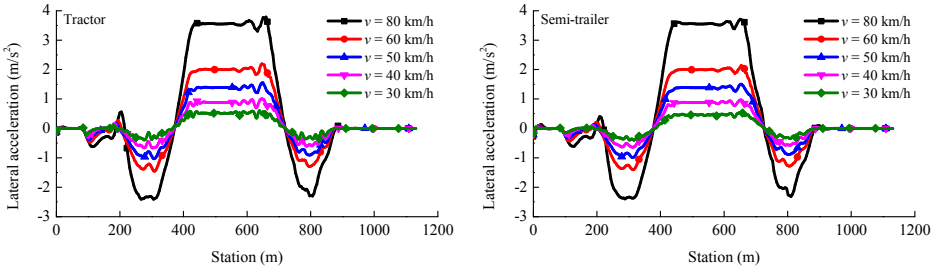

(b)

The roll angles of the articulated vehicle are shown in Figure 6. When the interchange is constructed without road bank involved, the roll angles increase with the increase of vehicle speed. The roll angle of the semi-trailer is a little greater than that of the tractor unit, and the maximum roll angle of the semi-trailer is 0.2° at the speed of 60 km/h on the circular curve with minimum road radius.

Figure 6 Roll angles (a) Neglecting road bank (b) With road bank considered

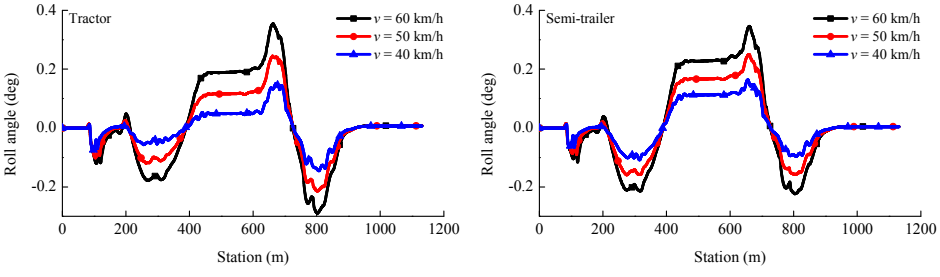

(a)

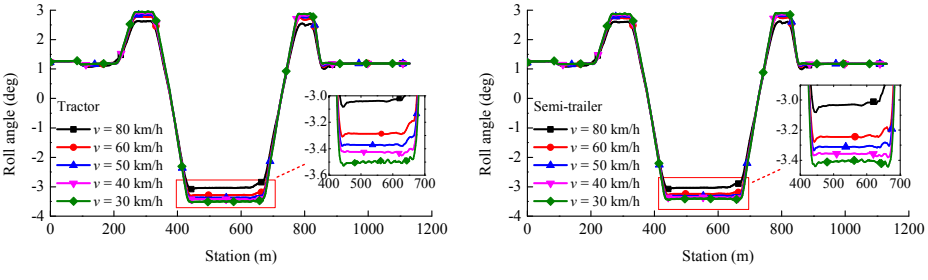

(b)

But actually, different bank angles are usually considered at the circular curves and transition curves on the ramp. Under this circumstance, the roll angle of the semi-trailer is a little smaller than the tractor's. The maximum roll angle of the semi-trailer is about –3.3° at the same speed on that road segment, as shown in Figure 6(b). This indicates the vehicle body rolls to the inside of the ramp. In addition, the roll angles increase with the decrease of running speed. It could be hypothesised that a heavy commercial vehicle at low speed might roll over to the inside of the large-banked curvature road.

The articulated vehicle is driven at a constant speed of 40 km/h, and applied a sharp reverse turn on the circular curve. The reverse turn here means turning the steering wheel towards the opposite direction of the road alignment. Figure 7 shows the animation of the articulated vehicle rollover to the inside of the ramp. These accidents occur during vehicle overtaking or obstacle avoidance on the curves. When suffered an emergency reverse turn on the curved road, the articulated vehicle might be driven onto a transverse slope. Under this situation, the centrifugal force of the vehicle and the lateral reaction force applied by the road both point to the inside of the curves, resulting in the vehicle rollover to the inside of the road.

Figure 7 Rollover to inside of the curved road

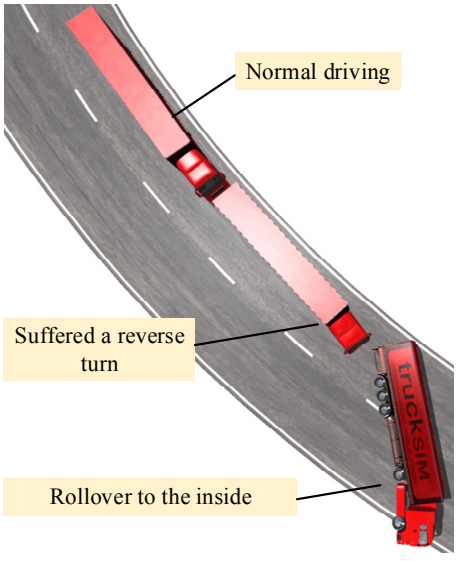

3.1.2 On ramp-D

Ramp-A and ramp-D are both exit ramps. But the road alignments are distinct, which results in different lateral accelerations. The articulated vehicle is driven upwards the ramp-D. When the station is located between 950 m and 1050 m, there is a circular curve with the minimum radius of 85 m. The lateral acceleration reaches the maximum value on this road segment, as shown in Figure 8. The peak lateral acceleration is considerably greater than that on the other ramps at the same speed because of the smallest radius of the circular curve. According to the identification method of vehicle sideslip proposed in the research (Zhao et al., 2015), the driving speed on the ramp-D should better not exceed 80 km/h to avoid sideslip risk.

Figure 8 Lateral acceleration on ramp-D

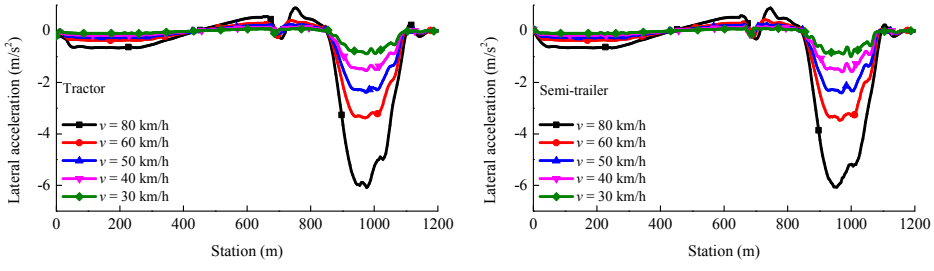

This ramp is short and the radius of the circular curve is rather small. Therefore, the length of the transition curve in front of the circular curve ought to be sufficient for deceleration. Warning signs at the ramp entrance and speed bumps on the transition curve should be set to remind drivers to slow down.

3.1.3 On ramp-C

The circular curve of ramp-C is relatively long, especially the one with the minimum road radius. The lateral acceleration on this road segment reaches the maximum and keep steady, as shown in Figure 9. The lateral acceleration reaches a negative peak at the last circular curve of the ramp. Transition curve in front of this circular curve is short compared with the others, which result in a sharp change of the lateral acceleration from positive to negative. This may cause discomfort and in adaptation of the driver during driving at a constant speed. Therefore, the transition curve connecting the continuous and reverse curvature roads should be long enough for the driver to adapt the change in the lateral acceleration to enhance driving safety and comfort.

Figure 9 Lateral acceleration on ramp-C

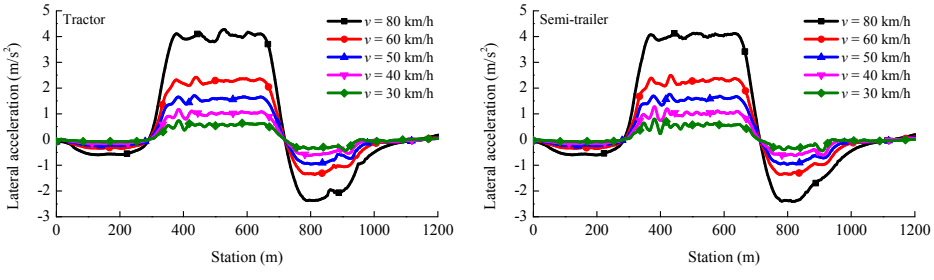

3.1.4 On ramp-B

Ramp-B is an entrance ramp, the same as the ramp-C. The ramp-B is mainly composed of a straight line and two minor-curvature transition curves coupled with a short circular curve. The lateral acceleration hold a low level and rapidly reaches the maximum at the circular curve if the vehicle is driving at a high speed without braking conducted on the straight line and the transition curve, as shown in Figure 10.

Figure 10 Lateral acceleration on ramp-B

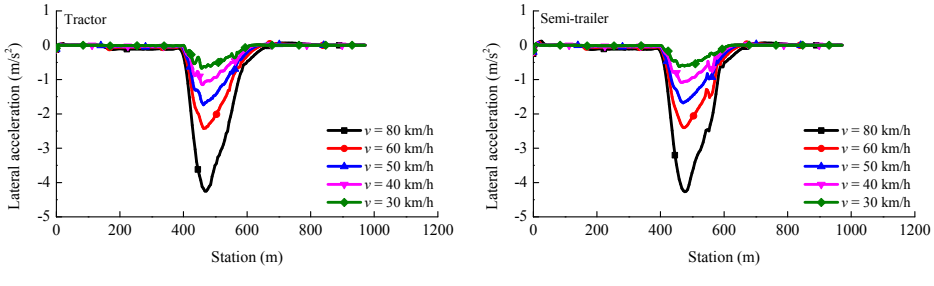

3.2 Effect of road friction

The road friction coefficient decreases too much on rainy days. To simulate the articulated vehicle travelling on wet roads, the friction coefficient is set as 0.3. In the

simulation, the vehicle is assigned to follow the road centreline. The animations and lateral distances to target path are individually presented in Figures 11 and 12.

Figure 11 Animations on ramps

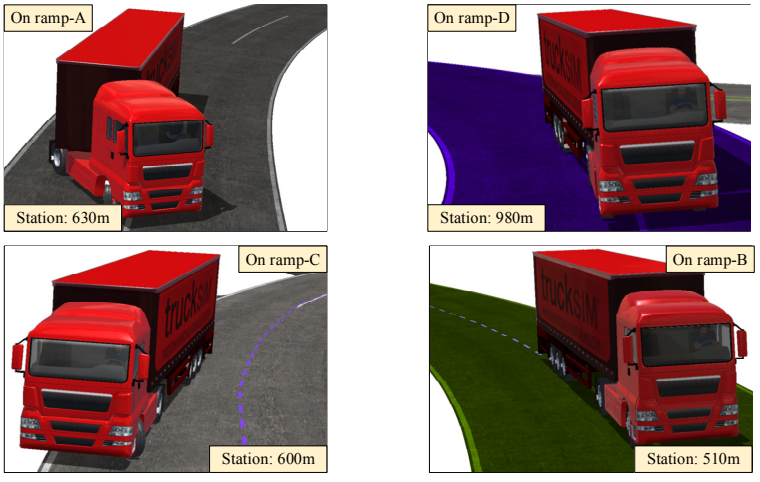

Figure 12 Lateral distances on ramps

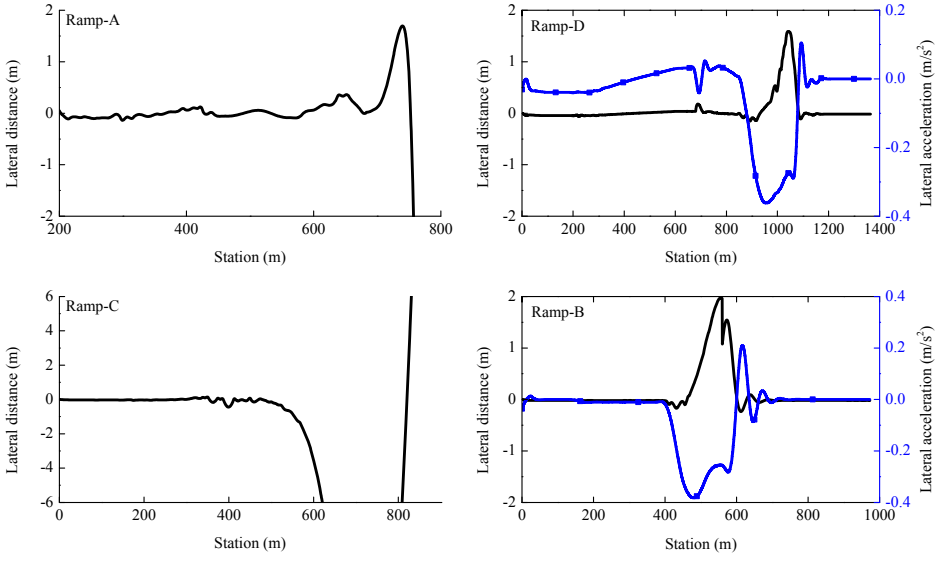

The articulated vehicle can be driven normally on the ramps at the speed of 60 km/h. However, the semi-trailer transversely skids at the speed of 78 km/h at the circular curve with the minimum radius on the ramp-A. This causes the actual trajectory of the tractor unit deviates obviously from the target path. The lateral distance to target path is more than half width of the ramp, which will result in tripped rollover because of transverse collision against the guardrail on the sides of the road.

The articulated vehicle is driving on the ramp-D at the speed of 62 km/h. The sideslip increases gradually after pulling into the circular curve and reaches the maximum. The peak lateral distance to the target path is 1.588 m. In the simulation, the vehicle is set to follow the road centreline. If driving on the left side of the ramp, the vehicle will pulls out of the lane due to the great sideslip. Strong shimmy of the trailer happens adjacent to the end of the transition curve.

While driving on the ramp-C at the speed of 75 km/h, tyres of articulated vehicle reach the adhesion limit. Sideslip occurs at the circular curve, and the tractor unit slips gradually out of the ramp together with the trailer.

The sideslip of the articulated vehicle is 0.522 m on the ramp-B at the driving speed of 77 km/h, while 2m at 78 km/h. The lateral distance to the target path is similar to that on the ramp-D. The sideslip reaches the maximum at the circular curve and the trailer shimmies strongly at the end of the transition curve.

4 Conclusions

Driving simulations are conducted to study the driving stability of the articulated vehicle on a typical interchange. Effects of running speed and road friction are analysed. The following conclusions are drawn. The lateral accelerations increase while roll angles decease with increased running speed on the transition and circular curves. The low-speed articulated vehicle suffered a sharply reverse turn might roll over to the inside of the large banked curves. Road friction limits the maximum driving speed on the road, and the safe speeds of the vehicle on the ramps are obtained.

Based on the simulations, the following risk preventions are proposed. For the ramp-D, the transition curve should be long enough for deceleration, and warning signs and speed bumps need to be set to remind drivers to slow down. For the ramp-C, the length of the transition curve used to connect the continuous and reverse curvature roads should be sufficient for the driver to adapt the change in the lateral acceleration.

Acknowledgements

The authors would like to thank anonymous reviewers for their helpful comments and suggestions to improve the manuscript. This research was supported by Natural Science Foundation Project of Chongqing in China (Grant No. cstc2021jcyj-msxmX0794), the Science and Technology Research Program of Chongqing Municipal Education Commission (Grant No. KJQN202000701), the Project of Innovative Research Groups for Universities in Chongqing (Grant No. CXQT21022) and the National Natural Science Foundation of China (Grant No. 52172340).

References

Brown, J., He, Y.P. and Lang, H.X. (2020) 'Quantifying drivers' driving skills using closed-loop dynamic simulations of articulated heavy vehicles', *Simulation Modelling Practice and Theory*, Vol. 99. Doi: 10.1016/j.simpat.2019.102014.

Calvi, A., Benedetto, A. and De Blasiis, M.R. (2015) 'Diverging driver performance along deceleration lanes: Driving simulator study', *Transportation Research Record*, Vol. 2518, pp.95–203.

Calvi, A., Benedetto, A., and De Blasiis, M.R. (2012) 'A driving simulator study of driver performance on deceleration lanes', *Accident Analysis and Prevention*, Vol. 45, pp.195–203.

Calvi, A., D'Amico, F., Ferrante, C. and Ciampoli, L.B. (2020) 'A driving simulator validation study for evaluating the driving performance on deceleration and acceleration lanes', *Advances in Transportation Studies*, Vol. 50, pp.67–80.

Ding. R., Liu, J., Jiang, Y. and Xu, J. (2021) 'Driving risks of interchange ramps based on vehicle acceleration data', *Journal of Transportation Information and Safety*, Vol. 39, No. 1, pp.17–25.

Dou, T.L., Xiang, J. and Xu, J. (2020a) 'Simulation research on driving safety and comfort of alfalfa leaf interchange', *Journal of Chinese Science and Technology Paper*, Vol. 15, No. 2, pp.201–207.

Dou, T.L., Xiang, J. and Xu, J. (2020b) 'Simulation research on driving safety and comfort of trumpet interchange', *Journal of Highway*, Vol. 5, pp.203–208.

Farah, H., Daamen, W. and Hoogendoorn, S. (2019) 'How do drivers negotiate horizontal ramp curves in system interchanges in the Netherlands?', *Safety Science*, Vol. 119, pp.58–69.

Farah, H., Van, B.A. and Daamen, W. (2017) 'Empirical speed behavior on horizontal ramp curves in interchanges in the Netherlands', *Transportation Research Record*, Vol. 2618, pp.38–47.

Hu, J.B., He, L.C. and Wang, R.H. (2020) 'Review of safety evaluation of freeway interchange', *China Journal of Highway Transport*, Vol. 33, No. 7, pp.17–27.

Kim, I. (2010) 'A safety evaluation method at freeway exit ramp based on driving behavior', *Proceedings of the 17th World Congress on Intelligent Transport Systems*, Busan, Korea.

Liu, L.N., Wang, J., Zhu, C.S. and Yang, Q. (2014) 'Study on the traffic behavior of on-ramp system considering driver behavior', *Proceedings of the International Conference on Materials Science and Computational Engineering*, Qingdao, China.

Livneh, M., Polus, A. and Factor, J. (1988) 'Vehicle behavior on deceleration lanes', *Journal of Transportation Engineering*, Vol. 114, No. 6, pp.706–717.

Luo, D.Y., Chen, J.Y., Wang, W.Y. and Wu, F. (2017) 'Simulation study on lane width of interchange ring ramp based on VISSIM', *Journal of East China Jiaotong University*, Vol. 34, No. 6, pp.33–37.

Lyu, N.C., Cao, Y., Wu, C.Z., Xu, J. and Xie, L. (2018) 'The effect of gender, occupation and experience on behavior while driving on a freeway deceleration lane based on field operational test data', *Accident Analysis and Prevention*, Vol. 121, pp.82–93.

Polus, A., Livneh, M. and Factor, J. (1985) 'Vehicle flow characteristics on acceleration lanes', *Journal of Transportation Engineering*, Vol. 111, No. 6, pp.595–606.

Portera, A. and Bassani, M. (2020) 'Factors influencing driver behavior along curved merging interchange terminals', *Transportation Research Part F Traffic Psychology and Behavior*, Vol. 75, pp.187–202.

Xu, J., Cui, Q., Chang, X., Fu, H.J, and Wu, G.X. (2019c) 'Longitudinal driving behavior characteristics at approaching / departing areas of clover leaf interchange', *Journal of Southeast University (Nature Science Edition)*, Vol. 49, No. 6, pp.1205–1214.

Xu, J., Cui, Q., Lin, W., Wang, D.Q. and Wu, G.X. (2019a) 'Speed behavior of passenger cars on helical ramps and helical bridges', *China Journal of Highway Transport,* Vol. 32, No. 7, pp.158–171.

Xu, J., Li, J.X., Lin, W., Cui, Q., Wu, G.X. and Yang, K. (2019b) 'Field Tests on lateral operational characteristics of passenger cars on helical ramps (bridges)', *Journal of Southwest Jiaotong University*, Vol. 54, No. 6, pp.1129–1138.

Zhao, S.E., Qu, X. and Zhang, J.L. (2015) 'Prediction of safe vehicle speed on curved roads based on driver-vehicle-road collaboration', *Automotive Engineering*, Vol. 37, No. 10, pp.1208–1214+1220.

Appendix

Variables and corresponding nomenclatures in the equations

Tractor	
Variables	*Notation*
u	Longitudinal velocity
δ	Steering angle
m_q	Total mass
m_{sq}	Sprung mass
β_q	Side slip angle
γ_q	Yaw rate
φ_q	Roll angle
h_{sq}	Height of sprung mass CG above the roll axis
h_{crq}	Height of hitch position above the roll axis
I_{zq}	Moment of inertia about z-axis
I_{xzq}	Product of inertia about x- and z-axis
I_{xsq}	Moment of inertia about x-axis of the sprung mass
a_1	Longitudinal distance from CG to the front axle
b_1	Longitudinal distance from CG to the rear axle
a_o	Longitudinal distance from CG to the hitch
K_q	Roll stiffness coefficient
C_q	Roll damping coefficient
K_{qb}	Roll stiffness coefficient of the hitch
F_{fq}	Lateral tyre force of the front axle
F_{rq}	Lateral tyre force of the rear axle
F_{qb}	Lateral hitch force
k_{fq}	Cornering stiffness of the front axle
k_{rq}	Cornering stiffness of the rear axle
α_{fq}	Slip angle of the front axle
α_{rq}	Slip angle of the rear axle

Appendix (continued)

Semi-trailer	
Variables	*Notation*
m_b	Total mass
m_{sb}	Sprung mass
β_b	Side slip angle
γ_b	Yaw rate
φ_b	Roll angle
h_{sb}	Height of sprung mass CG above the roll axis
h_{crb}	Height of hitch position above the roll axis
I_{zb}	Moment of inertia about z-axis
I_{xzb}	Product of inertia about x- and z-axis
I_{xsb}	Moment of inertia about x-axis of the sprung mass
b_1	Longitudinal distance from CG to the front axle
b_o	Longitudinal distance from CG to the hitch
K_b	Roll stiffness coefficient
C_b	Roll damping coefficient
F_b	Lateral tyre force of the rear axle
k_b	Cornering stiffness of the rear axle
α_b	Slip angle of the rear axle